Article

Luminescent Device for Detection of Oxidative Stress Biomarker in Artificial Urine

Gopal Ammanath, Umit Hakan Yildiz, Alagappan Palaniappan, and Bo Liedberg

ACS Appl. Mater. Interfaces, **Just Accepted Manuscript** • DOI: 10.1021/acsami.7b17252 • Publication Date (Web): 12 Feb 2018

Luminescent Device for Detection of Oxidative Stress Biomarker in Artificial Urine

Gopal Ammanath [a,b,c], Umit Hakan Yildiz [d], Alagappan Palaniappan [a,c*], Bo Liedberg [a,b,c,*]

a. Center for Biomimetic Sensor Science, Nanyang Technological University, Singapore 639798

b. Nanyang Institute of Technology in Health and Medicine, Interdisciplinary Graduate School, Nanyang Technological University, Singapore 637553

c. School of Materials Science and Engineering, Nanyang Technological University, Singapore 639798,

d. Department of Chemistry, Izmir Institute of Technology, Urla, 35430 Izmir, Turkey

E-mail: alps@ntu.edu.sg; bliedberg@ntu.edu.sg

ABSTRACT

A luminescent paper device for visual detection of oxidative stress biomarker is reported. The assay platform consists of a polyvinylidene fluoride (PVDF) membrane impregnated with poly(3-alkoxy-4-methylthiophene) (PT) for colorimetric sensing. 8-hydroxy-2'-deoxyguanosine (8-OHdG), a biomarker associated with oxidative stress, is used as a model system for validating the proposed methodology. The sensing strategy is based on monitoring the changes in optical properties of PT associated with its conformational changes upon interaction with an aptamer in the presence and in the absence of 8-OHdG. Spectral characterization revealed linear responses for 8-OHdG concentrations between 50 pM to 500 nM (~14 pg/ml to 140 ng/ml), with a limit of detection of ~ 300 pM for (n=3). Colorimetric responses in artificial urine ascertained rapid, sensitive, and selective detection of 8-OHdG at clinically relevant (pM to nM) concentration levels. Furthermore, the proposed methodology enables point of care diagnostics for oxidative stress without requiring sophisticated instrumentation.

Keywords: Paper-based biosensor, naked eye detection, polythiophene, artificial urine, oxidative stress, 8-OHdG.

INTRODUCTION

Reactive oxygen species (ROS) are chemically active oxygen containing molecules that are produced as byproducts of various physiological, metabolic and biochemical processes. While low levels of ROS aid cell signal transduction and immune response, an increase in their steady-state levels causes oxidative stress [1-2]. Subsequent imbalance in oxidants and anti-oxidants in the normal redox state of the cells produces peroxides and free radicals that damage proteins, lipids, carbohydrates and nucleic acids [3-4]. The damage in these molecules causes cell death and progresses to various diseases like cancer, neurodegenerative disorders, cardiovascular disease, inflammatory disease and diabetes mellitus [5-6]. The elevated oxidative stress levels is therefore a precursor state in these diseases [5]. Thus, the detection of oxidative stress related biomarkers could assist in the early diagnosis as well as for monitoring of disease progression.

ROS induced oxidation results in formation of numerous DNA fragments. Among them, 8-hydroxy-2'-deoxyguanosine (8-OHdG) is a repaired product of oxidative guanine lesions and an important biomarker for oxidative stress. Thus, the assay of 8-OHdG helps in early detection of diseases such as diabetes, cancer and neurodegenerative disorders [7-8]. 8-OHdG has been quantified in various biological samples such as urine, saliva, blood and tissue [9-12]. Reports indicate that the average levels of 8-OHdG are ~20 ng/ml and ~ 80 ng/ml in healthy and diseased subjects, respectively, thereby requiring sensitive methodologies for their assay [11, 13].

The most commonly used analytical techniques for the detection of 8-OHdG in urine are high performance liquid chromatography-electrochemical detection (HPLC-ECD) [14], HPLC tandem mass spectrometry (HPLC MS/MS) [15], capillary electrophoresis with electrochemical detection (CE-ECD) [12, 16], electrochemical methods including cyclic voltammetry (CV) [17-19],

differential pulse voltammetry [20] and linear sweep voltammetry (LSV) [21]. Ultraviolet spectroscopy [22-23], fluorescence spectroscopy [24-25], resonance light scattering (RLS) [26] and enzyme-linked immunosorbent assay (ELISA) [27] have also been explored for the detection of 8-OHdG. However, most of them are laboratory techniques requiring sophisticated instrumentation and trained personnel to perform the assay. Thus, it is highly desirable to develop a point of care (POC) assay for 8-OHdG. Over the recent years, the concept of paper based sensing has gained significant attention for fabrication of lab-on-a-chip devices enabling point of care analysis [28-32]. Although paper based biosensors for 8-OHdG analysis have been reported, most of the approaches involve antibodies, which pose stability concerns [33-34]. In this context, a paper based colorimetric assay for POC 8-OHdG assay utilizing aptamers is proposed.

The proposed device comprises of a PVDF membrane, a filter paper and lamination sheets. Cationic polythiophene (PT), with triethylamine pendant groups, is utilized for colorimetric reporting due to its superior optical and electronic properties [35-37]. Herein, PT is impregnated in the PVDF membrane along with an aptamer as the 8-OHdG recognition element. A guanine-rich aptamer sequence, reported to exhibit a high affinity for 8-OHdG, is utilized in this study [38]. As illustrated in Figure 1, the sensing strategy is based on monitoring the changes in optical properties of PT associated with its conformational changes upon interaction with the aptamer in the presence and in the absence of 8-OHdG, respectively. Complexation of PT-aptamer in the PVDF membrane produces a duplex due to the electrostatic interactions between PT and the aptamer. These interactions induce fluorescence quenching resulting in a color transition from orange (PT) to purple (PT-aptamer). The color transition of PT is not observed in the presence of 8-OHdG as complexation is perturbed yielding fluorescent PT-aptamer-8-OHdG complexes, owing to the affinity between aptamer and 8-OHDG. Therefore, the orange color

(PT-aptamer-8-OHdG) and the significantly different purple color (PT-aptamer) correspond to the presence and the absence of 8-OHdG, respectively, thereby enabling naked eye detection of 8-OHdG. The assay of 8-OHdG yielded a linear colorimetric response for clinically relevant concentration ranges between 50 pM and 500 nM with a limit of detection of ~ 350 pM, enabling point of care detection without requiring sophisticated instrumentation.

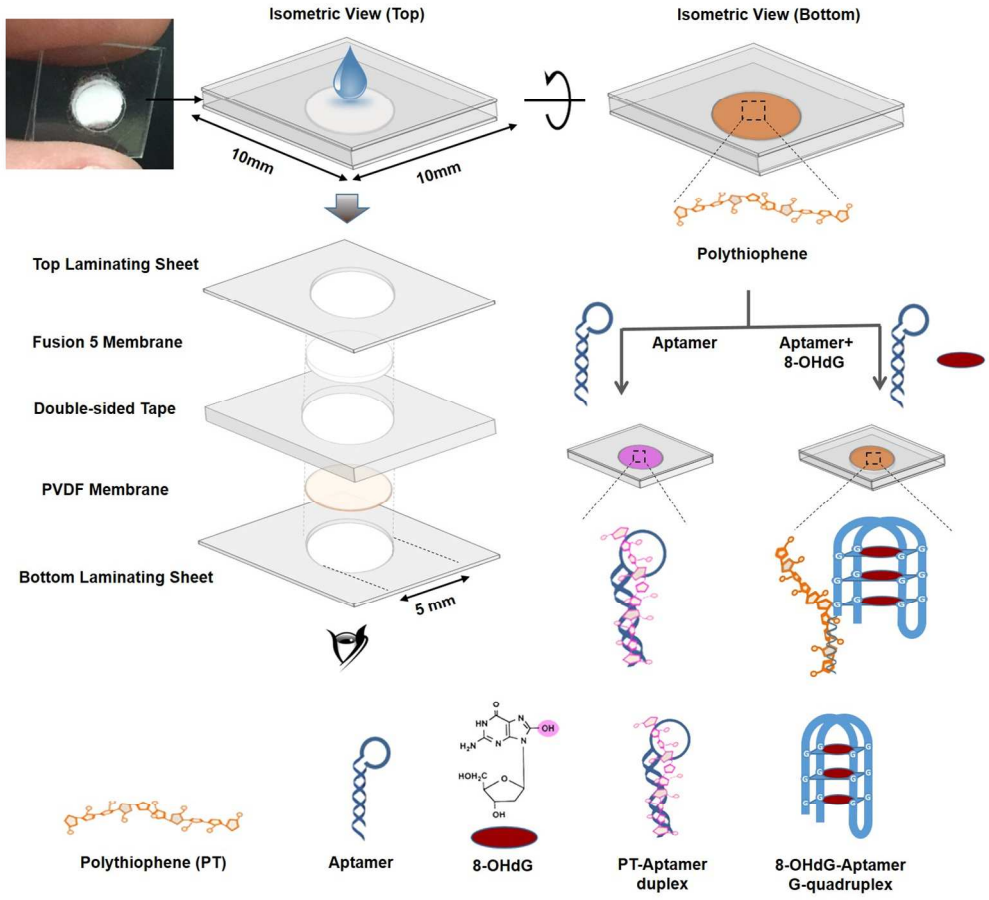

Figure 1: Schematic representation of the luminescent paper device illustrating distinguishable colorimetric responses of poly(3-alkoxy-4-methylthiophene) (PT) for the G-quadruplex-secondary structure of aptamer in the presence of 8-OHdG and for the PT-aptamer duplex in the absence of 8-OHdG.

EXPERIMENTAL SECTION

Materials and Chemicals

8-OHdG, artificial (synthetic) urine and all the reagents and solvents were obtained from Sigma-Aldrich and used without further purification. The 8-OHdG aptamer (sequence, 5′–GCG GGC GAT CGG CGG GGG GTG CGT GCG CTC TGT GCC AGG GGG TGG GAC AGA TCA TAT GGG GGT GCT–3′) [38], was synthesized by IDT, Singapore followed by PAGE purification. PVDF centrifugation tubes of 0.1 μm pore size were purchased from Merck. Fusion 5 membranes made of glass fibers were purchased from Whatman and used for the pretreatment of samples.

Synthesis, Sample Preparation and Analysis

A water soluble PT was synthesized by oxidative polymerization of its monomer (m1) using the protocol reported previously [39]. The protocol adopted for synthesis of m1 and PT and their corresponding NMR spectra are provided in supporting information Figure S1. NMR spectra were recorded using a Bruker Advance 400 MHz spectrometer. In brief, 200 μL of 5 μM PT was added to a centrifugation tube. Tubes were centrifuged at 8000 rpm for 3 min. The above step was repeated for 3 more times. After impregnation of PT, the PVDF membranes were washed twice using DI water at 8000 rpm for 3 min and dried overnight. PVDF membranes deposited with PT was then peeled off from the centrifugation tube for device fabrication.

A vertical flow-through configuration was adopted for its advantages over the lateral-flow format in terms of low sample volume and decreased assay time. Capillary or passive forces allow this system to operate without the requirement of an external pump [40]. The device consisted of 2 laminated sheets containing a FUSION 5 filter paper and a PVDF membrane impregnated with PT for colorimetric sensing (Figure 1). The lamination sheets containing FUSION 5 and PVDF paper were then attached using a double-sided adhesive tape.

PVDF membrane impregnated with PT was then incubated with 1 μM aptamer followed by addition of varying concentrations of 8-OHdG (~5 μL). To ascertain the obtained color changes, the devices were placed on a UV illumination zone (portable UV lamp, at 365 nm, 8 W) and digital images were captured using a Sony Xperia Z5 premium mobile phone camera positioned at a fixed distance from the device. Subsequently, the digital images were transferred to a computer as jpeg files for image processing. The raw images were imported into "ImageJ" software and the centroids of paper membranes (75 × 75 pixels) were utilized to create a digital array. The RGB values were evaluated using ImageJ software in order to ascertain colorimetric responses. The process of creating color-coded digital array is shown in Figure S2. Fluorescence measurements were performed using Avantes spectrofluorometer and the emission spectra were recorded for analysis.

RESULTS AND DISCUSSION

Interaction of PT with aptamer and 8-OHdG

The assay for naked eye detection of 8-OHdG is based on monitoring the changes in optical properties of PT upon complexation with the aptamer in the presence and in the absence of 8-OHdG. The aptamer utilized for affinity binding to 8-OHdG with K_d value of 0.1 μmol L^{-1} [38] was modified by removing the primer 1 and primer 2 sequences at the 3′ and 5′ in order to serve as an effective recognition element for proposed assay. 5 μM PT and 1 μM aptamer (in DI water) were determined to be the optimum concentrations for monitoring 8-OHdG at clinically relevant levels (pM to nM). Figure 2a illustrates that addition of 1 μM aptamer onto the PT-impregnated PVDF membrane yields a color change from orange (PT on PVDF membrane) to purple (PT-aptamer complex on PVDF membrane), column 1 to column 2. The duplex formation is associated with backbone planarization and aggregation of the PT due to the electrostatic

interactions between the positively charged PT (associated with the triethylamine groups) and the negatively charged aptamer. These electrostatic interactions cause a change from a random-coiled morphology of PT to a planar π-stacking morphology, leading to a substantial quenching of the fluorescence signal and a concomitant color transition. Saturated colorimetric response for 8-OHdG is expected to overlap with the color of PT, provided complete 8-OHDG-aptamer complex formation and consequent weakening of electrostatic interaction between PT and aptamer, whereas assay concentrations would yield intermediate colorimetric responses between columns one and two depending on the strength of interaction between the PT and the aptamer. Therefore for the assay, different concentrations of 8-OHdG from 50 pM to 500 nM were added to the PT impregnated PVDF membranes containing the aptamer. 8-OHdG induces a conformational change of the aptamer containing a Guanine-rich nucleic acid sequence to form G-quadruplex structures as shown in Figure 1. The formation of the rigid structure of G-quadruplex reduces the electrostatic interactions between PT and aptamer, thereby leading to fluorescence and color recovery of PT. Figure 2 a,b illustrates that both color change and fluorescence recovery occur with increasing concentration of 8-OHdG, attributed to the formation of a G-quadruplex structures. Decreasing 8-OHdG concentration changes the color from orange to purple as shown in Figure 2a. The two significantly different optical signals (PT-aptamer and PT-aptamer-8-OHdG) are subsequently analyzed and correlated to the concentration of 8-OHDG. Figure 2a shows a 75x75 pixel color-coded digital array of various concentration of 8-OHdG (500 nM to 50 pM, left to right) for subsequent analysis.

In order to validate the assay, fluorescence spectra were recorded for the PT-aptamer incorporated PVDF membranes for various concentrations of 8-OHdG. Upon excitation at 420 nm, an emission maxima centered at 566 nm with a shoulder at around 625 nm appeared as

shown in Figure 2b. The spectrum of the PT impregnated paper is red shifted (about 25 nm) with respect to the solution spectrum likely because of partial self-aggregation/confinement of PT [35, 41-42]. Even though aggregation causes loss in fluorescence intensity, the PT impregnated paper shows clearly visible orange color emission upon UV exposure (365 nm), as illustrated in Figure 2a. Moreover, steady state fluorescence spectroscopy reveals a substantial quenching in emission and red shift (about 15 nm) upon addition of aptamer (black to red) indicating a duplex formation between PT and aptamer. As observed from Figure 2b, the fluorescence intensity gradually increases with the increasing concentration of 8-OHdG due to the formation 8-OHdG-aptamer G-quadruplex complexes. Further evidence of complex formation is obtained from the RGB analysis of the color-coded digital array (Figure 2c) via ImageJ software. As shown in Figure 2c, there is a substantial change in the G (from 150.3 to 68.4) and B (from 76.9 to 129.1) values upon addition of aptamer to PT, whereas upon addition of 500 nM 8-OHdG with the aptamer, the G (118.2) and B (74.5) values reverts back to that of PT indicating almost complete recovery of color. It could be observed that the G (from 118.2 to 63) and B (from 74.5 to 119.7) values decreases and increases, respectively, with the decreasing concentrations of 8-OHdG. In order to ensure reproducibility, spectral and RGB analysis of the impregnated paper were conducted for three independent assays. Figure 2c shows that RGB analysis is in agreement with the naked eye observation (Figure 2a). The correlation between 8-OHdG concentration and normalized fluorescence intensity is evaluated using the ratio I/I_{PT}, where I and I_{PT} represents the integrated fluorescence intensity from 450 nm to 750 nm for the assay and PT, respectively. The linearity of the response was analyzed using a semi logarithmic plot of normalized fluorescence intensity

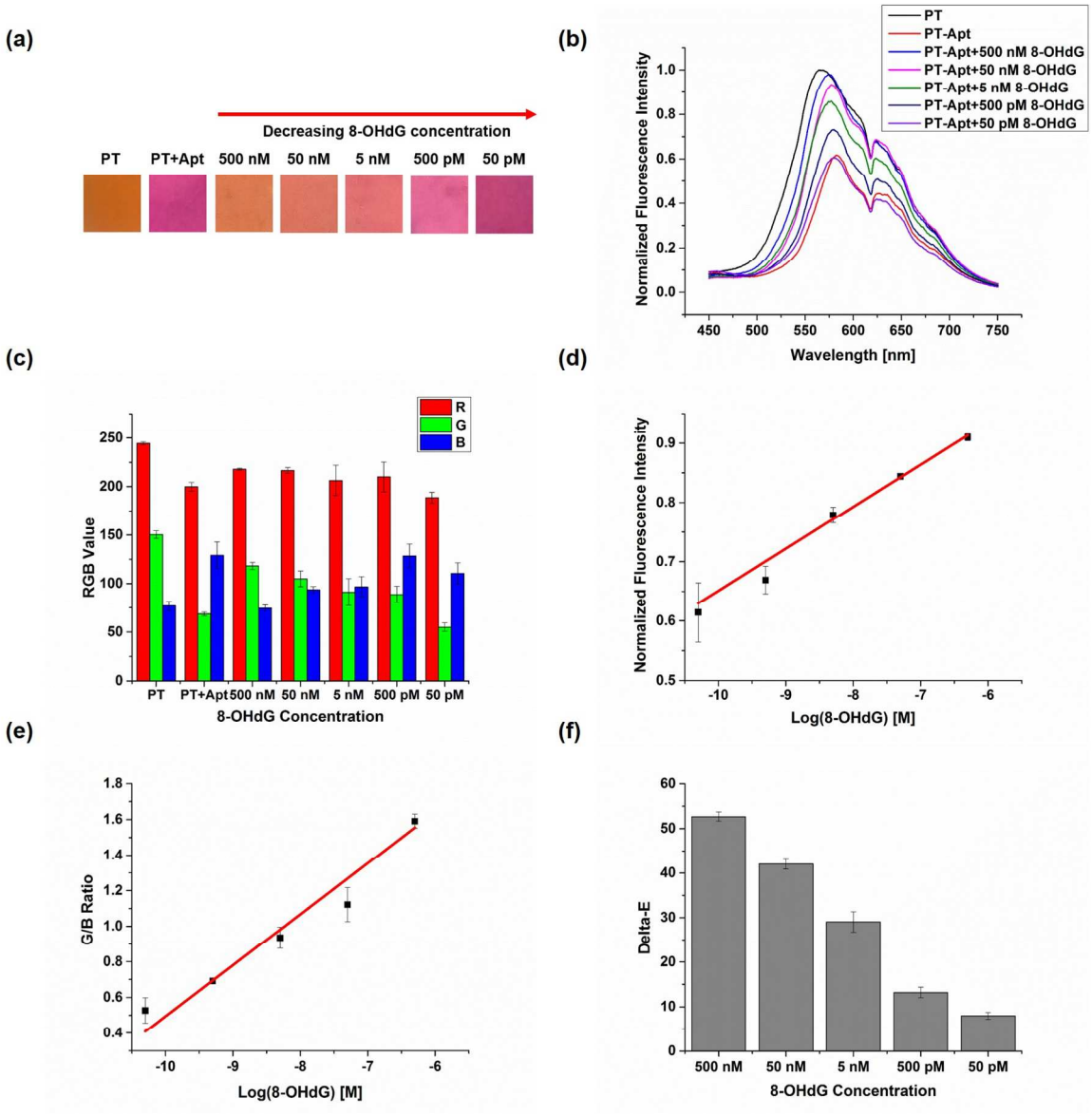

Figure 2: (a) Color-coded digital array of PT with aptamer and various 8-OHdG concentrations. (b) Normalized fluorescence spectra upon addition of aptamer and various concentrations of 8-OHdG (c) mean RGB values and standard deviation for n=3 (d) Semilogarithimic plot of 8-OHdG concentration versus normalized fluorescence intensity and the corresponding linear fit (e) Semilogarithimic plot of 8-OHdG concentration versus ratio of G/B values and the corresponding linear fit (f) mean delta E values and standard deviation for (n=3) of various 8-OHdG concentrations with respect to PT-aptamer.

versus concentration of 8-OHdG. Figure 2d shows the linear regression equation (Y= 0.0767logX+1.3998, R^2= 0.989, n=3), yielding a limit of detection of ~300 pM (S/N=3).

Similarly, the correlation between concentration of 8-OHdG and colorimetric response is evaluated using the G and B values from the Figure 2c. The linearity of the response was ascertained by a semi logarithmic plot of G/B ratio versus 8-OHdG concentration (n=3), as shown in Figure 2e with a linear regression equation of (Y=0.2557logX+3.0955, R^2=0.96, n=3) yielding a limit of detection of ~350 pM (S/N=3). Furthermore, Delta-E values, ranging between 0-100, is a metric for human eye perception of color differences, is calculated using International Commission of Illumination (CIE) 1976 algorithm [43]. Figure 2f illustrates a broad range of delta E (~from 8 to 53) for PT-aptamer-8-OHdG and PT-aptamer in the assay concentration range of 8-OHDG (50 pM to 500 nM), indicating that the color difference between PT-aptamer-8-OHdG and PT-aptamer could be visually distinguished.

Selectivity studies

The selectivity of the platform was evaluated using metal ions, potentially interfering compounds and other 8-OHdG analogues that may coexist in urine. As observed from Figure 3a, the metal ions, analogues and the interfering compounds yield almost similar visual responses (varying shades of purple) as that of the aptamer, whereas, 50 nM 8-OHdG with and without interfering molecules show a recovery of color to orange from purple. Figure 3b shows the fluorescence recovery of 8-OHdG, metal ions and other interfering compounds. The fluorescence recovery was calculated as $(I-I_{aptamer})/(I_{PT}-I_{aptamer})$, where $I_{aptamer}$ represents the integrated fluorescence intensity of PT-aptamer complex from 450 nm to 750 nm. Small to negligible fluorescence recovery is observed upon addition of 8-OHdG analogues and metal ions, even at 100 times higher concentration than that of 8-OHdG, Figure 3b. The higher concentrations of

ions such as potassium and 8-OHdG analogues interfere with the detection of 8-OHdG (maximum of ~20 % for potassium) as observed from Figure 3b suggesting that these molecules could also induce a conformational change of the aptamer [22]. However, such ions could be eliminated from the sample matrices by dialysis using a dialysis bag with a molecular weight cut off (MWCO) of 200 Da. In the mixture of 50 nM 8-OHdG with 8-OHdG analogues and interfering compounds such as guanosine, guanine, uric acid, ascorbic acid and cytosine, a recovery around 64% was observed as against 67% for 50 nM 8-OHdG without interfering compounds, illustrating excellent selectivity of the proposed methodology.

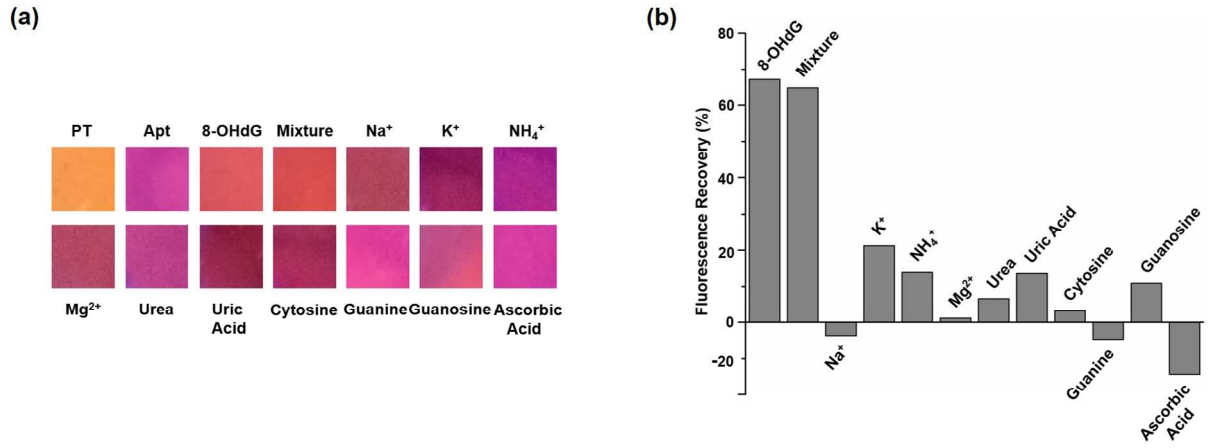

Figure 3: (a) Color coded digital array of proposed platform with 8-OHdG and interfering molecules (b) Fluorescence recovery upon addition of 8-OHdG, metal ions, 8-OHdG analogues and other potentially interfering compounds (Mixture: 8-OHdG with interfering compounds such as uric acid, cytosine, guanine, guanosine and ascorbic acid)

Analysis in Artificial Urine

In order to validate the proposed methodology for clinical applications, different concentrations of 8-OHdG were spiked in the synthethic urine and tested. As shown in Figure 4a, varying colorimetric responses are obatained upon addition of different concentrations of 8-

OHdG in spiked urine. The orange PT color appears realtively darker upon addition of artificial urine samples without aptamer and there is a reduction of the fluoresence intensity, as compared to that of DI water. A possible explanation is that other anions in artificial urine might contibute to the formation of planar π-stacking morphology upon electrostatic interactions with PT and thereby lowering the PT fluorescence. However, as shown in column 2 in Figure 4a, the color changes to purple upon addition of aptamer, which is in agreement with the responses in DI.

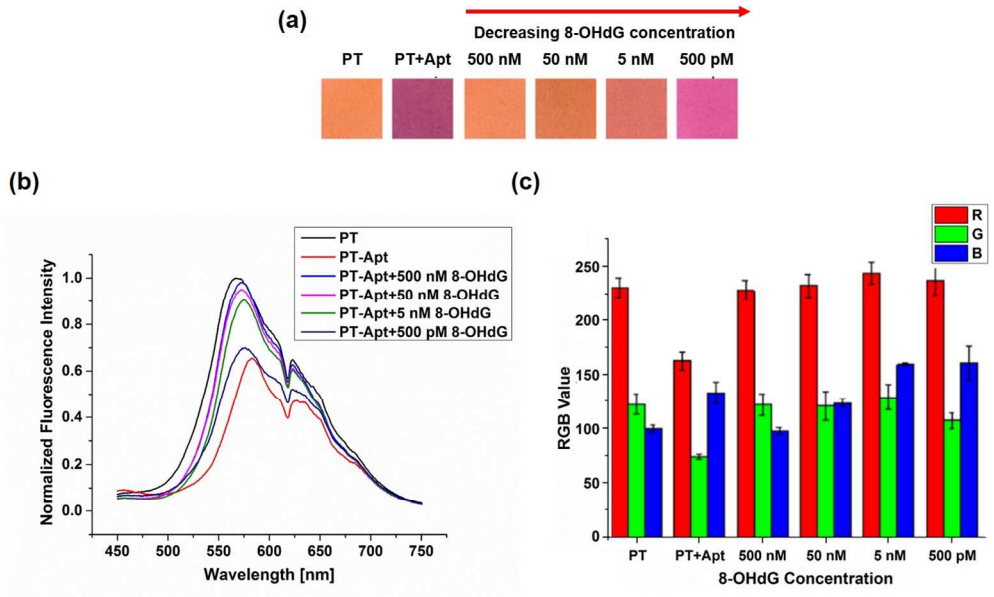

Figure 4: (a) Color coded digital array of PT with aptamer and various 8-OHdG concentrations in artificial urine (b) Normalized fluorescence spectra upon addition of aptamer and various 8-OHdG concentrations (c) mean RGB values and standard deviation for n=3.

A color change from orange to pink was observed upon decreasing the concentration of 8-OHdG from 500 nM to 500 pM (left to right in Figure 4a). As shown in Figure 4b there is also a substantial quenching of fluorescence upon addition of the aptamer (black to red) and the fluorescence intensity recovers gradually with increasing 8-OHdG concentration (from 500 pM to 500 nM). Further evidence of 8-OHdG aptamer complex formation is obtained from the RGB

analysis, Figure. 4c. Upon addition of aptamer there is a significant change of RGB values from PT to PT-aptamer (orange to purple) whereas upon addition of 500 nM 8-OHdG, the RGB values almost reverts back to PT, indicating the change in color from purple to orange. Changes in RGB values were also observed with varying concentrations of 8-OHdG. Figure 4c shows that RGB analysis is in agreement with naked eye observation and the proposed methodology can be used for the detection of 8-OHdG at clinically relevant concentration ranges in urine samples. It should be noted that the responses were recorded using synthetic urine at a pH of 6.7 and at temperatures ranging between 10 ºC and 40 ºC. The influence of temperature, pH and light shown in Figures S3 and S4, respectively, suggests that acidic pH (<6) might cause interference in sensor response and that the samples should be stored in dark. Operation of paper-based assay is not recommended above 40 ºC.

Comparison with other sensing strategies

Electrochemical methodologies such as cyclic voltammetry (CV) and differential pulse voltammetry (DPV) for quantitative analysis of 8-OHdG have claimed subnanomolar detection sensitivities [17, 20]. Similarly, spectroscopic methods such as ultraviolet-visible spectroscopy (UV-Vis) and fluorescence spectroscopy have also been explored for the detection of 8-OHdG [22-24] with subnanomolar and picomolar sensitivities. However, most of the reported methodologies involve tedious and sophisticated assay protocols. Table 1 illustrates that the LOD of the proposed methodology is either better or comparable to previous reports, while exhibiting a wider linear dynamic range for 8-OHdG detection. Our findings indicate a linear response for both color and the fluorescence intensity for clinically relevant concentration ranges of 8-OHdG (50 pM to 500 nM) [13] with a limit of detection of ~ 350 pM and 300 pM, respectively.

Table 1: Comparison of various sensing platforms for the detection of 8-OHdG

Methodology	Detection Range	Limit of detection (LOD)	Ref.
LSV	0.7−70 µM	100 nM	[21]
DPV	0.5−35 µM	31.3 nM	[20]
CV	0.0563-16.4 µM	18.8 nM	[19]
CV	5.6−1155 nM	0.875 nM	[17]
CE-ECD	0.01-1.5 µM	2.6 nM	[16]
UV−vis	5.6−282 nM	1.7 nM	[22]
UV-vis	0.466-247 nM	141 pM	[23]
Colorimetric and Electrochemical	35.3-706.1 nM	7.3 nM	[34]
Fluorescence	3.96-211 nM	1.19 nM	[24]
Colorimetric and Fluorescence	0.5-500 nM	~ 350 pM Colorimetric and ~ 300 pM Fluorescence	Reported methodology

In addition, the overall detection processes is conducted at ambient conditions and the experimental procedure is facile. Furthermore, the proposed methodology possesses significant advantages over conventional sensing platforms such as ease of use, ease of fabrication and low cost with an assay time of 30 min.

Conclusions

A disposable paper based analytical device for the naked eye detection of oxidative stress is reported. The proposed methodology has been validated for 8-OHdG assay using luminescent reporter (PT) impregnated PVDF membranes. The obtained colorimetric responses in artificial urine indicate the potential for use in clinical applications for early diagnosis of various diseases associated with reactive oxygen species. The fabricated platform could be ideal for point-of-care applications and for detection of oxidative stress at locations where sophisticated instrumentation is sparse or even nonexistent. Future studies will emphasize on

detection of 8-OHdG in patient samples, optimization of device storage conditions, development of assay for other potential ROS markers and bench marking with established methodologies.

Supporting Information

Synthesis protocol and the NMR spectra for the precursors/monomer and PT, color coded array creation process for RGB analysis, influence of temperature and pH on 8-OHdG assay, influence of light, degree of polymerization and GMP on PT.

Acknowledgments:

The authors wish to acknowledge funding support from Tier 1 MOE - RG 82/12, and NITHM M4081989.070.500000 research grants. The authors further wish to thank Profs. Ali Yusuf and Bernhard Boehm LKC School of Medicine, Nanyang Technological University, for fruitful discussions.

References

(1) Semchyshyn, H. M.; Lushchak, V. I. Interplay Between Oxidative and Carbonyl Stresses: Molecular Mechanisms, Biological Effects and Therapeutic Strategies of Protection. In *Oxidative Stress-Molecular Mechanisms and Biological Effects*; InTech: 2012.

(2) Kivatinitz, S. C. Relationship Between Protein Oxidation Markers and Oxidative Stress Biomarkers, Inflammatory Diseases. In *Immunopathology, Clinical and Pharmacological Bases*; InTech: 2012.

(3) Dalle-Donne, I.; Giustarini, D.; Colombo, R.; Rossi, R.; Milzani, A. Protein Carbonylation in Human Diseases. *Trends in molecular medicine* **2003,** *9* (4), 169-176.

(4) Niedworok, J.; Fijałkowski, P. Effect of Long-Term Aluminium Chloride Intoxication on Selected Biochemical Parameters and Oxidative--Antioxidative Balance in Experimental Animals. *Polish Journal of Environmental Studies* **2004,** *13* (1), 41-43.

(5) Lowe, F. Biomarkers of Oxidative Stress. In *Systems Biology of Free Radicals and Antioxidants*; Springer: 2014; pp 65-87.

(6) Dalle-Donne, I.; Rossi, R.; Colombo, R.; Giustarini, D.; Milzani, A. Biomarkers of Oxidative Damage in Human Disease. *Clinical chemistry* **2006,** *52* (4), 601-623.

(7) Valavanidis, A.; Vlachogianni, T.; Fiotakis, C. 8-Hydroxy-2'-Deoxyguanosine (8-OHdG): A Critical Biomarker of Oxidative Stress and Carcinogenesis. *Journal of environmental science and health Part C* **2009,** *27* (2), 120-139.

(8) Kasai, H. Analysis of a form of Oxidative DNA Damage, 8-Hydroxy-2'-Deoxyguanosine, As a Marker of Cellular Oxidative Stress During Carcinogenesis. *Mutation Research/Reviews in Mutation Research* **1997,** *387* (3), 147-163.

(9) Subash, P.; Gurumurthy, P.; Sarasabharathi, A.; Cherian, K. Urinary 8-OHdG: A Marker of Oxidative Stress to DNA and Total Antioxidant Status in Essential Hypertension with South Indian Population. *Indian Journal of Clinical Biochemistry* **2010,** *25* (2), 127-132.
(10) Guan, Y.; Zhou, G.; Ye, J. Fast Quantification of Salivary 8-Hydroxy-2′-Deoxyguanosine as DNA Damage Biomarker Using CE with Electrochemical Detection. *Chromatographia* **2014,** *77* (7-8), 603-607.
(11) Bolner, A.; Pilleri, M.; De Riva, V.; Nordera, G. Plasma and Urinary HPLC-ED Determination of the Ratio of 8-OHdG/2-dG in Parkinson's Disease. *Clinical laboratory* **2011,** *57* (11), 859.
(12) Arnett, S. D.; Osbourn, D. M.; Moore, K. D.; Vandaveer, S. S.; Lunte, C. E. Determination of 8-Oxoguanine and 8-Hydroxy-2′-Deoxyguanosine in the Rat Cerebral Cortex Using Microdialysis Sampling and Capillary Electrophoresis with Electrochemical Detection. *Journal of Chromatography B* **2005,** *827* (1), 16-25.
(13) Cutler, R. G.; Rodriguez, H. *Critical Reviews of Oxidative Stress and Aging: Advances in Basic Science, Diagnostics and Intervention*, World Scientific: 2003; Vol. 2.
(14) Koide, S.; Kinoshita, Y.; Ito, N.; Kimura, J.; Yokoyama, K.; Karube, I. Determination of Human Serum 8-hydroxy-2′-deoxyguanosine (8-OHdG) by HPLC-ECD Combined with Solid Phase Extraction (SPE). *Journal of Chromatography B* **2010,** *878* (23), 2163-2167.
(15) Weimann, A.; Belling, D.; Poulsen, H. E. Quantification of 8-Oxo-Guanine and Guanine as the Nucleobase, Nucleoside and Deoxynucleoside Forms in Human Urine by High-Performance Liquid Chromatography–Electrospray Tandem Mass Spectrometry. *Nucleic acids research* **2002,** *30* (2), e7-e7.
(16) Zhang, S. W.; Zou, C. J.; Luo, N.; Weng, Q. F.; Cai, L. S.; Wu, C. Y.; Xing, J. Determination of Urinary 8-Hydroxy-2′-Deoxyguanosine by Capillary Electrophoresis with Molecularly Imprinted Monolith in-Tube Solid Phase Microextraction. *Chinese Chemical Letters* **2010,** *21* (1), 85-88.
(17) Jia, L.-P.; Liu, J.-F.; Wang, H.-S. Electrochemical Performance and Detection of 8-Hydroxy-2′-Deoxyguanosine at Single-Stranded DNA Functionalized Graphene Modified Glassy Carbon Electrode. *Biosensors and Bioelectronics* **2015,** *67*, 139-145.
(18) Gutiérrez, A.; Gutiérrez, S.; García, G.; Galicia, L.; Rivas, G. A. Determinatiom of 8-Hydroxy 2′-Deoxyguanosine Using Electrodes Modified with a Dispersion of Carbon Nanotubes in Polyethylenimine. *Electroanalysis* **2011,** *23* (5), 1221-1228.
(19) Guo, Z.; Liu, X.; Liu, Y.; Wu, G.; Lu, X. Constructing a Novel 8-Hydroxy-2′-Deoxyguanosine Electrochemical Sensor and Application in Evaluating the Oxidative Damages of DNA and Guanine. *Biosensors and Bioelectronics* **2016,** *86*, 671-676.
(20) Sun, X.; Zhang, L.; Zhang, H.; Qian, H.; Ji, J.; Tang, L.; Li, Z.; Zhang, G. Electrochemical detection of 8-Hydroxy-2′-Deoxyguanosine as a Biomarker for Oxidative DNA Damage in HEK293 Cells Exposed to 3-Chloro-1, 2-Propanediol. *Analytical Methods* **2015,** *7* (16), 6664-6671.
(21) Li, T.-H.; Jia, W.-L.; Wang, H.-S.; Liu, R.-M. Electrochemical Performance Of 8-Hydroxy-2′-Deoxyguanosine and its Detection at Poly (3-methylthiophene) Modified Glassy Carbon Electrode. *Biosensors and Bioelectronics* **2007,** *22* (7), 1245-1250.
(22) Wang, J.-C.; Wang, Y.-S.; Rang, W.-Q.; Xue, J.-H.; Zhou, B.; Liu, L.; Qian, Q.-M.; Wang, Y.-S.; Yin, J.-C. Colorimetric Determination of 8-Hydroxy–2′-Deoxyguanosine Using Label-Free Aptamer and Unmodified Gold Nanoparticles. *Microchimica Acta* **2014,** *181* (9-10), 903-910.
(23) Liu, H.; Wang, Y.-S.; Wang, J.-C.; Xue, J.-H.; Zhou, B.; Zhao, H.; Liu, S.-D.; Tang, X.; Chen, S.-H.; Li, M.-H. A Colorimetric Aptasensor for the Highly Sensitive Detection of 8-Hydroxy-2′-Deoxyguanosine Based on G-Quadruplex–Hemin Dnazyme. *Analytical biochemistry* **2014,** *458*, 4-10.
(24) Liu, H.; Wang, Y.-S.; Tang, X.; Yang, H.-X.; Chen, S.-H.; Zhao, H.; Liu, S.-D.; Zhu, Y.-F.; Wang, X.-F.; Huang, Y.-Q. A Novel Fluorescence Aptasensor for 8-Hydroxy-2′-Deoxyguanosine Based on the Conformational Switching of K^+-Stabilized G-Quadruplex. *Journal of pharmaceutical and biomedical analysis* **2016,** *118*, 177-182.

(25) Dou, K.; Chen, G.; Yu, F.; Liu, Y.; Chen, L.; Cao, Z.; Chen, T.; Li, Y.; You, J. Bright and Sensitive Ratiometric Fluorescent Probe Enabling Endogenous FA Imaging and Mechanistic Exploration of Indirect Oxidative Damage due to FA In Various Living Systems. *Chemical science* **2017,** *8* (11), 7851-7861.
(26) Wang, J.-C.; Wang, Y.-S.; Xue, J.-H.; Zhou, B.; Qian, Q.-M.; Wang, Y.-S.; Yin, J.-C.; Zhao, H.; Liu, H.; Liu, S.-D. An Ultrasensitive Label-Free Assay of 8-Hydroxy-2'-Deoxyguanosine Based on the Conformational Switching of Aptamer. *Biosensors and Bioelectronics* **2014,** *58*, 22-26.
(27) Wu, L. L.; Chiou, C.-C.; Chang, P.-Y.; Wu, J. T. Urinary 8-OHdG: A Marker of Oxidative Stress to DNA and a Risk Factor for Cancer, Atherosclerosis And Diabetics. *Clinica Chimica Acta* **2004,** *339* (1), 1-9.
(28) Fu, X.; Cheng, Z.; Yu, J.; Choo, P.; Chen, L.; Choo, J. A SERS-Based Lateral Flow Assay Biosensor for Highly Sensitive Detection of HIV-1 DNA. *Biosensors and Bioelectronics* **2016,** *78*, 530-537.
(29) Sun, M.; Johnson, M. A. Measurement of Total Antioxidant Capacity in sub-µl Blood Samples Using Craft Paper-Based Analytical Devices. *RSC advances* **2015,** *5* (69), 55633-55639.
(30) Dungchai, W.; Sameenoi, Y.; Chailapakul, O.; Volckens, J.; Henry, C. S. Determination of Aerosol Oxidative Activity Using Silver Nanoparticle Aggregation on Paper-Based Analytical Devices. *Analyst* **2013,** *138* (22), 6766-6773.
(31) Liana, D. D.; Raguse, B.; Gooding, J. J.; Chow, E. Recent Advances in Paper-Based Sensors. *Sensors* **2012,** *12* (9), 11505-11526.
(32) Parolo, C.; Merkoçi, A. Paper-Based Nanobiosensors for Diagnostics. *Chemical Society Reviews* **2013,** *42* (2), 450-457.
(33) Martins, G. V.; Tavares, A. P.; Fortunato, E.; Sales, M. G. F. Paper-Based Sensing Device for Electrochemical Detection of Oxidative Stress Biomarker 8-Hydroxy-2'-deoxyguanosine (8-OHdG) in Point-of-Care. *Scientific Reports* **2017,** *7*, 14558.
(34) Zhu, X.; Shah, P.; Stoff, S.; Liu, H.; Li, C.-z. A Paper Electrode Integrated Lateral Flow Immunosensor for Quantitative Analysis of Oxidative Stress Induced DNA Damage. *Analyst* **2014,** *139* (11), 2850-2857.
(35) Ho, H.-A.; Najari, A.; Leclerc, M. Optical Detection of DNA and Proteins with Cationic Polythiophenes. *Accounts of chemical research* **2008,** *41* (2), 168-178.
(36) Lee, K.; Povlich, L. K.; Kim, J. Recent Advances in Fluorescent and Colorimetric Conjugated Polymer-Based Biosensors. *Analyst* **2010,** *135* (9), 2179-2189.
(37) Zade, S. S.; Bendikov, M. Twisting of Conjugated Oligomers and Polymers: Case Study of Oligo-and Polythiophene. *Chemistry–A European Journal* **2007,** *13* (13), 3688-3700.
(38) Miyachi, Y.; Shimizu, N.; Ogino, C.; Fukuda, H.; Kondo, A. Selection of a DNA Aptamer that Binds 8-OHdg Using GMP-Agarose. *Bioorganic & medicinal chemistry letters* **2009,** *19* (13), 3619-3622.
(39) Rajwar, D.; Ammanath, G.; Cheema, J. A.; Palaniappan, A.; Yildiz, U. H.; Liedberg, B. Tailoring Conformation-Induced Chromism of Polythiophene Copolymers for Nucleic Acid Assay at Resource Limited Settings. *ACS applied materials & interfaces* **2016,** *8* (13), 8349-8357.
(40) Vella, S. J.; Beattie, P.; Cademartiri, R.; Laromaine, A.; Martinez, A. W.; Phillips, S. T.; Mirica, K. A.; Whitesides, G. M. Measuring Markers of Liver Function Using a Micropatterned Paper Device Designed for Blood from a Fingerstick. *Analytical chemistry* **2012,** *84* (6), 2883-2891.
(41) Yildiz, U. H.; Alagappan, P.; Liedberg, B. Naked Eye Detection of Lung Cancer Associated miRNA by Paper Based Biosensing Platform. *Analytical chemistry* **2012,** *85* (2), 820-824.
(42) Ho, H.-A.; Leclerc, M. Optical Sensors Based on Hybrid Aptamer/Conjugated Polymer Complexes. *Journal of the American Chemical Society* **2004,** *126* (5), 1384-1387.
(43) Hill, B.; Roger, T.; Vorhagen, F. W. Comparative Analysis of the Quantization of Color Spaces on the Basis of the CIELAB Color-Difference Formula. *ACM Transactions on Graphics (TOG)* **1997,** *16* (2), 109-154.

Table of Contents Graphic